Supplemental Information for

A hierarchical assembly pathway directs the unique subunit arrangement of TRiC/CCT

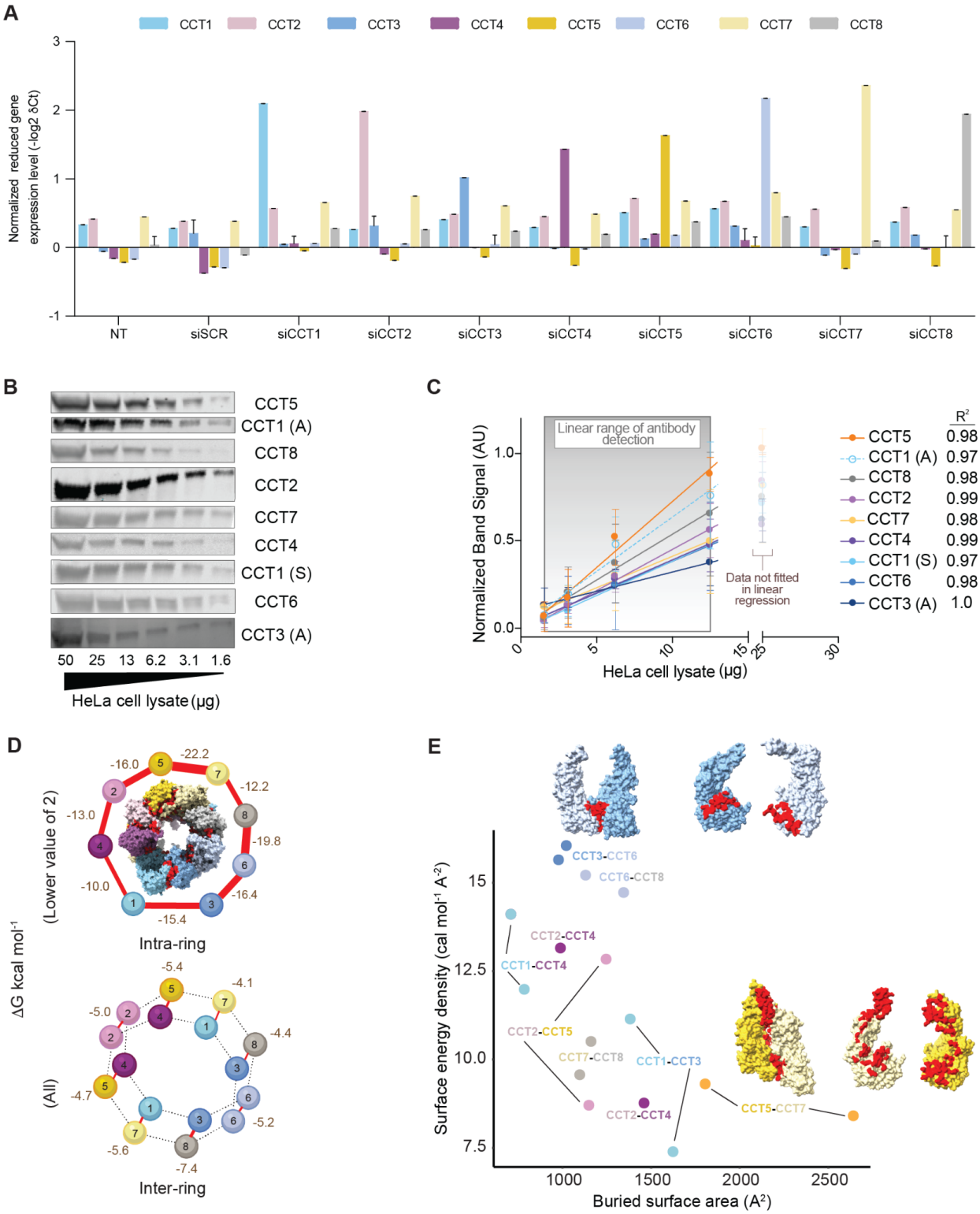
A
CCT1
CCT2
CCT3
CCT4
CCT5
CCT6
CCT7
CCT8
Normalized reduced gene expression level (-log2 δCt)
NT
siSCR
siCCT1
siCCT2
siCCT3
siCCT4
siCCT5
siCCT6
siCCT7
siCCT8
B
CCT5
CCT1 (A)
CCT8
CCT2
CCT7
CCT4
CCT1 (S)
CCT6
CCT3 (A)
50 25 13 6.2 3.1 1.6
HeLa cell lysate (µg)
C
Linear range of antibody detection
Data not fitted in linear regression
Normalized Band Signal (AU)
HeLa cell lysate (µg)
R²
CCT5 0.98
CCT1 (A) 0.97
CCT8 0.98
CCT2 0.99
CCT7 0.98
CCT4 0.99
CCT1 (S) 0.97
CCT6 0.98
CCT3 (A) 1.0
D
ΔG kcal mol⁻¹
(Lower value of 2)
Intra-ring
(All)
Inter-ring
E
Surface energy density (cal mol⁻¹ A⁻²)
Buried surface area (A²)
CCT3-CCT6
CCT6-CCT8
CCT2-CCT4
CCT1-CCT4
CCT2-CCT5
CCT7-CCT8
CCT1-CCT3
CCT2-CCT4
CCT5-CCT7

Figure S1. Validation of RNA depletion and protein quantitation of CCT subunits and structural analysis of CCT interfaces. Related to Figure 1.

A. qPCR quantification of CCT RNA levels in HeLa cells treated with siRNA targeting each subunit or SCR (scrambled) control, related to protein level measurements in Figures 1 and 2. Error bars represent SD of the mean (n = 3). **B.** Representative immunoblots for determining linearity of CCT detection in HeLa lysate for CCT antibodies used in this study. A = Abcam, S = Santa Cruz Biotechnology. **C.** Correlation between protein levels and signal intensity of Western blot bands for CCTs and linear regression analysis of selected measurements to determine linearity of antibody detection in **B**. Error bars represent SD of the mean (n = 3). **D.** PISA predictions of the lowest free energy of formation ΔG (kcal mol^{-1}) for intra-ring (top) and inter-ring (bottom) interfaces within open-state TRiC (PDB: 7WU7). Interface residues are colored red in the structure and width of red lines are proportional to estimated ΔG values. **E.** Surface energy density of each intra-ring CCT-CCT interface based on PISA analysis of TRiC. Burying a given unit of surface area confers more energetic benefit for smaller interfaces, and this benefit plateaus for the largest interfaces, primarily CCT5-CCT7. This trend is also observed in the proteome generally[1]. Structures show intact and side views of interfaces with the highest and lowest surface energy densities with participating residues in red.

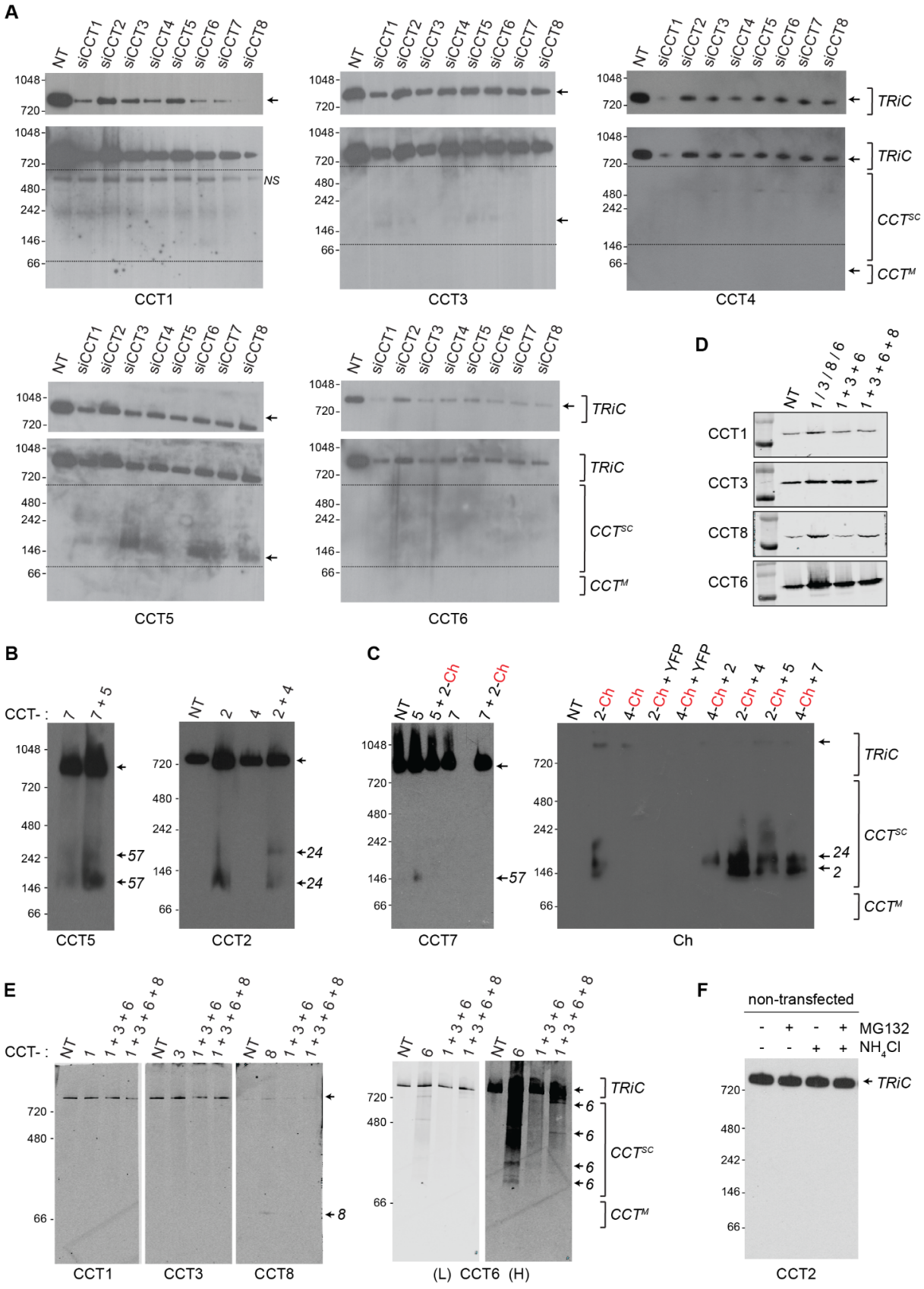
A
NT
siCCT1
siCCT2
siCCT3
siCCT4
siCCT5
siCCT6
siCCT7
siCCT8
1048
720
480
242
146
66
NS
TRiC
CCT^SC
CCT^M
CCT1
CCT3
CCT4
CCT5
CCT6
D
1 / 3 / 8 / 6
1 + 3 + 6
1 + 3 + 6 + 8
CCT1
CCT3
CCT8
CCT6
B
CCT- :
7
7 + 5
2
4
2 + 4
57
24
CCT5
CCT2
C
5
5 + 2-Ch
7 + 2-Ch
2-Ch
4-Ch
2-Ch + YFP
4-Ch + YFP
4-Ch + 2
2-Ch + 4
2-Ch + 5
4-Ch + 7
CCT7
Ch
E
1
3
8
6
(L) CCT6 (H)
F
non-transfected
MG132
NH4Cl
CCT2

Figure S2. CCT subcomplexes form in cells between CCT2, CCT4, CCT5, and CCT7, but not CCT1, CCT3, CCT6, and CCT8. Related to Figure 2.

A. NativePAGE immunoblots of HeLa cells after individual CCT knockdowns. Low exposure blots (top) are shown to visualize TRiC depletion; higher exposure blots (bottom) highlight subcomplexes (*CCT*^{sc}) or monomers (*CCT*^{M}). Blots for all CCT subunits not in Figure 2 are shown. NT = non-transfected. A non-specific (NS) band is recognized by the CCT1 antibody. **B.** Subcomplexes between assembly partners CCT2-CCT4 and CCT5-CCT7 are detected by NativePAGE immunoblots after co-overexpression in HeLa cells without tags. **C.** Overexpression in HeLa cells with non-paired subunits and non-CCT controls. Left: CCT7 is not appreciably detected in subcomplexes without concomitant overexpression of CCT5. Right: CCT2 and CCT4 are enriched in subcomplexes upon overexpression with other early-assembling CCTs in addition to each other, and are not enriched in subcomplexes when co-overexpressed with YFP (yellow fluorescent protein). **D.** SDS-PAGE confirms increased protein levels of CCT1, CCT3, CCT6, and CCT8 in HeLa cells upon their overexpression alone or together. **E.** NativePAGE immunoblots for CCT1, CCT3, CCT6, and CCT8 after their overexpression alone or together in HeLa cells. No subcomplexes containing two or more of these subunits are detected. The only species smaller than TRiC observed in these experiments are a faint CCT8 monomer, and laddering of CCT6 high molecular weight oligomers at high blot exposure (right). **F.** NativePAGE immunoblot for CCT2 in HeLa cells after treatment with proteasome inhibitor MG132 and/or autophagy inhibitor NH_4Cl, as an additional control against experiments in Figure 2D. All overexpression was done by transient transfection.

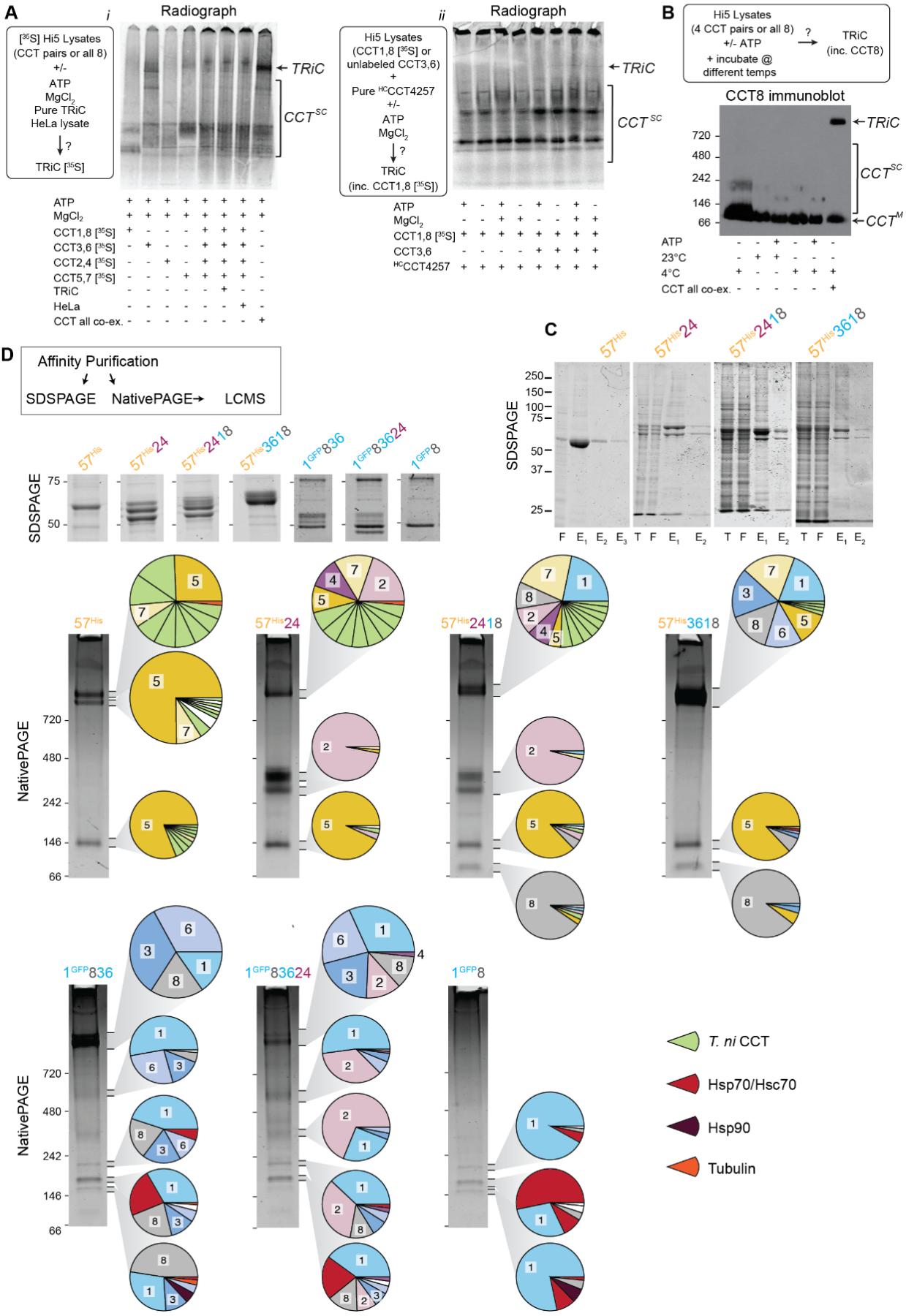
A
i
Radiograph
[35S] Hi5 Lysates
(CCT pairs or all 8)
+/-
ATP
MgCl2
Pure TRiC
HeLa lysate
?
TRiC [35S]
TRiC
CCTSC
ATP
MgCl2
CCT1,8 [35S]
CCT3,6 [35S]
CCT2,4 [35S]
CCT5,7 [35S]
TRiC
HeLa
CCT all co-ex.
ii
Radiograph
Hi5 Lysates
(CCT1,8 [35S] or
unlabeled CCT3,6)
+
Pure HCCCT4257
+/-
ATP
MgCl2
?
TRiC
(inc. CCT1,8 [35S])
TRiC
CCTSC
ATP
MgCl2
CCT1,8 [35S]
CCT3,6
HCCCT4257
B
Hi5 Lysates
(4 CCT pairs or all 8)
+/- ATP
+ incubate @
different temps
?
TRiC
(inc. CCT8)
CCT8 immunoblot
720
480
242
146
66
TRiC
CCTSC
CCTM
ATP
23°C
4°C
CCT all co-ex.
C
57His
57His24
57His2418
57His3618
SDSPAGE
250
150
100
75
50
37
25
F E1 E2 E3 T F E1 E2 T F E1 E2 T F E1 E2
D
Affinity Purification
SDSPAGE
NativePAGE
LCMS
57His
57His24
57His2418
57His3618
1GFP836
1GFP83624
1GFP8
75
50
720
480
242
146
66
T. ni CCT
Hsp70/Hsc70
Hsp90
Tubulin

Figure S3. Recombinant CCTs assemble into various complexes dependent on their co-expression and cannot form TRiC post-hoc. Related to Figure 3.

A. NativePAGE and ^{35}S radiography testing for TRiC assembly in diverse lysates. The indicated CCTs were expressed in Hi5 cells and lysates expressing pairs were mixed or co-expressed. (i) TRiC = addition of purified human TRiC. HeLa = addition of mammalian cell lysate. (ii) ^{HC}CCT4257 = Purified complex. **B.** NativePAGE and CCT8 immunoblot testing for TRiC assembly at two temperatures +/- ATP. Four Hi5 lysates each expressing a different CCT pair were mixed prior to incubation at the indicated temperature. TRiC was only observed when CCTs were co-expressed. **C.** SDS-PAGE following steps of His-affinity purification of different CCT co-expression combinations from Hi5 cells. T = total lysate, F = flow-through, E = elution(s). **D.** SDS-PAGE after affinity purification from Hi5 cells. **E.** Summary of analyses of CCT complexes after affinity purification using the His-tag on CCT7 (top row) or GFP on CCT1 (bottom row). Coomassie-stained bands were excised from NativePAGE and subjected to in-gel protease digestion and LCMS. Circles show all components constituting over 1% of each band by relative iBAQ.

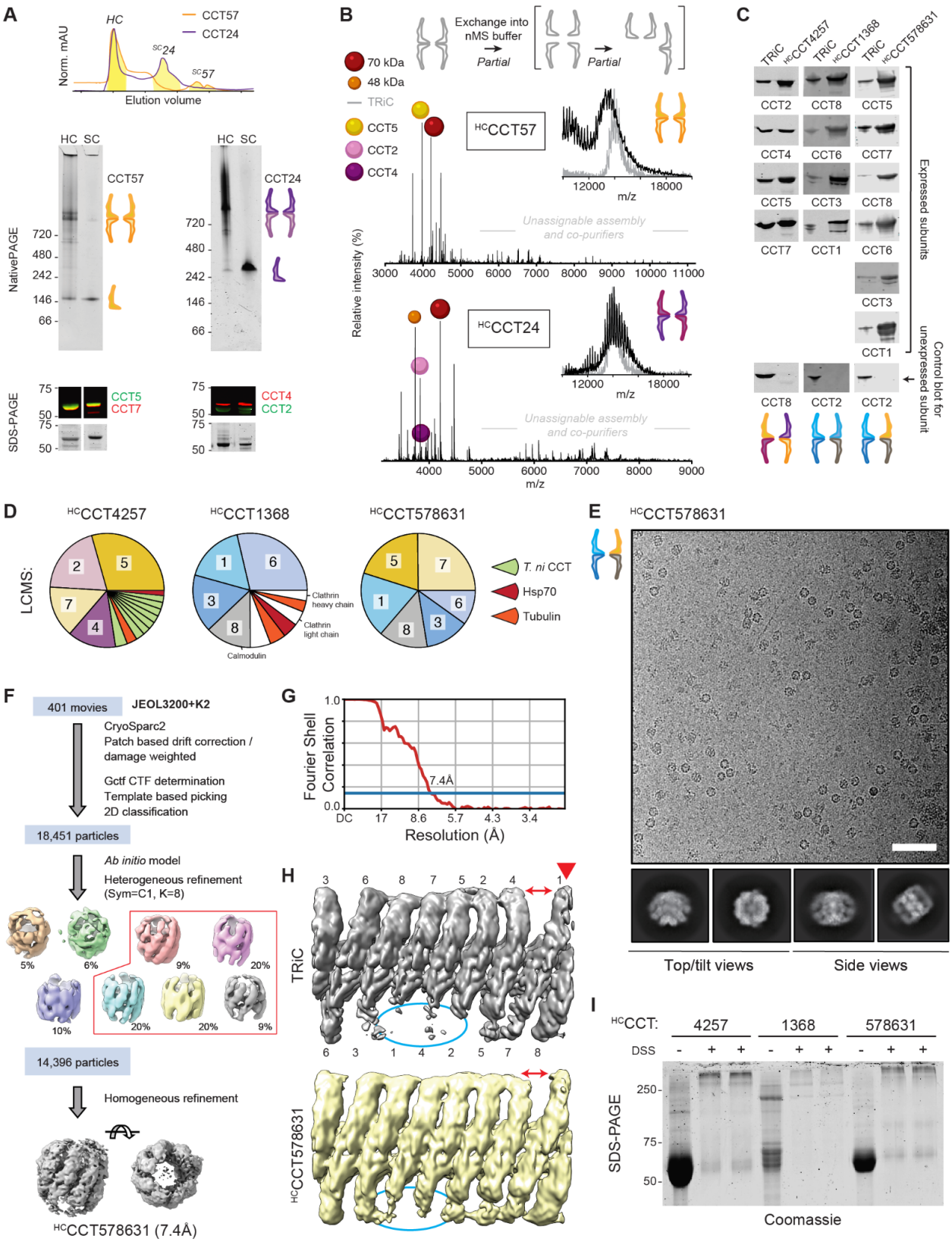
A
HC
CCT57
CCT24
Norm. mAU
SC24
SC57
Elution volume
HC SC
CCT57
CCT24
NativePAGE
720
480
242
146
66
SDS-PAGE
75
50
CCT5
CCT7
CCT4
CCT2
B
Exchange into nMS buffer
Partial
Partial
70 kDa
48 kDa
TRiC
CCT5
CCT2
CCT4
HCCCT57
12000
18000
m/z
Unassignable assembly and co-purifiers
Relative intensity (%)
3000 4000 5000 6000 7000 8000 9000 10000 11000
HCCCT24
12000
18000
m/z
Unassignable assembly and co-purifiers
4000 5000 6000 7000 8000 9000
m/z
C
TRiC
HCCCT4257
TRiC
HCCCT1368
TRiC
HCCCT578631
CCT2 CCT8 CCT5
CCT4 CCT6 CCT7
CCT5 CCT3 CCT8
CCT7 CCT1 CCT6
CCT3
CCT1
Expressed subunits
Control blot for unexpressed subunit
CCT8 CCT2 CCT2
D
HCCCT4257
HCCCT1368
HCCCT578631
LCMS:
2 5 7 4
1 6 3 8
Clathrin heavy chain
Clathrin light chain
Calmodulin
5 7 1 6 3 8
T. ni CCT
Hsp70
Tubulin
E
HCCCT578631
Top/tilt views
Side views
F
401 movies
JEOL3200+K2
CryoSparc2
Patch based drift correction / damage weighted
Gctf CTF determination
Template based picking
2D classification
18,451 particles
Ab initio model
Heterogeneous refinement
(Sym=C1, K=8)
5%
6%
9%
20%
10%
20%
20%
9%
14,396 particles
Homogeneous refinement
HCCCT578631 (7.4Å)
G
Fourier Shell Correlation
1.0
0.0
7.4Å
DC 17 8.6 5.7 4.3 3.4
Resolution (Å)
H
TRiC
3 6 8 7 5 2 4 1
6 3 1 4 2 5 7 8
HCCCT578631
I
HCCCT:
4257
1368
578631
DSS
- + + - + + - + +
SDS-PAGE
250
75
50
Coomassie

Figure S4. Characterization of TRiC-like complexes assembled from CCT subsets. Related to Figure 4.

A. Size exclusion chromatography of co-expressed CCT5/CCT7 or CCT2/CCT4 and analysis of the resulting holocomplexes (HC) and subcomplexes (SC). Complexes were purified from Hi5 lysate by nickel resin prior to SEC, with affinity mediated by a His-tag on CCT7 or by intrinsic nickel affinity of CCT2. ^{HC}CCT57 is more monodisperse than ^{HC}CCT24; and both HCs partially dissociate into SCs post-SEC. Immunoblots confirm the presence of both subunits in all complexes, and total protein staining suggests they are not present in equimolar amounts. **B.** Native mass spectrometry of ^{HC}CCT57 and ^{HC}CCT24. Insets show HC signals compared to a mass spectrum of TRiC. Lower mass charge series are assignable to CCT monomers as well as putative Hsp70 and a 48 kDa contaminant mass from ^{HC}CCT24 that may be tubulin. The remainder of both mass spectra contain an array of oligomers we could not conclusively assign. **C.** Immunoblots of HCs confirm the presence of all co-expressed subunits and absence of one unexpressed subunit (red outline) in each complex. All bands shown are between 50 and 75 kDa molecular weight markers. **D.** Summary of proteomic analyses of HCs, showing all components constituting over 1% of each sample by relative iBAQ. **E.** Representative electron micrograph of ^{HC}CCT578631 with 2-D class averages on the right. Scale bar = 50 nm. **F.** CryoEM image processing workflow for map refinement. **G.** Map resolution for ^{HC}CCT578631 according to the Fourier shell correlation (FSC) at 0.143 criterion. **H.** Unwrapped 3D maps showing overall subunit architecture of TRiC and ^{HC}CCT578631. The red arrowhead indicates the protruding subunit (CCT1 in TRiC) creating an asymmetric gap feature between apical domains that is shared between the structures. Blue circled areas denote flexible apical regions. **I.** Differential SDS-PAGE mobilities support that treatment with cross-linking agent DSS prevents holocomplex dissociation.

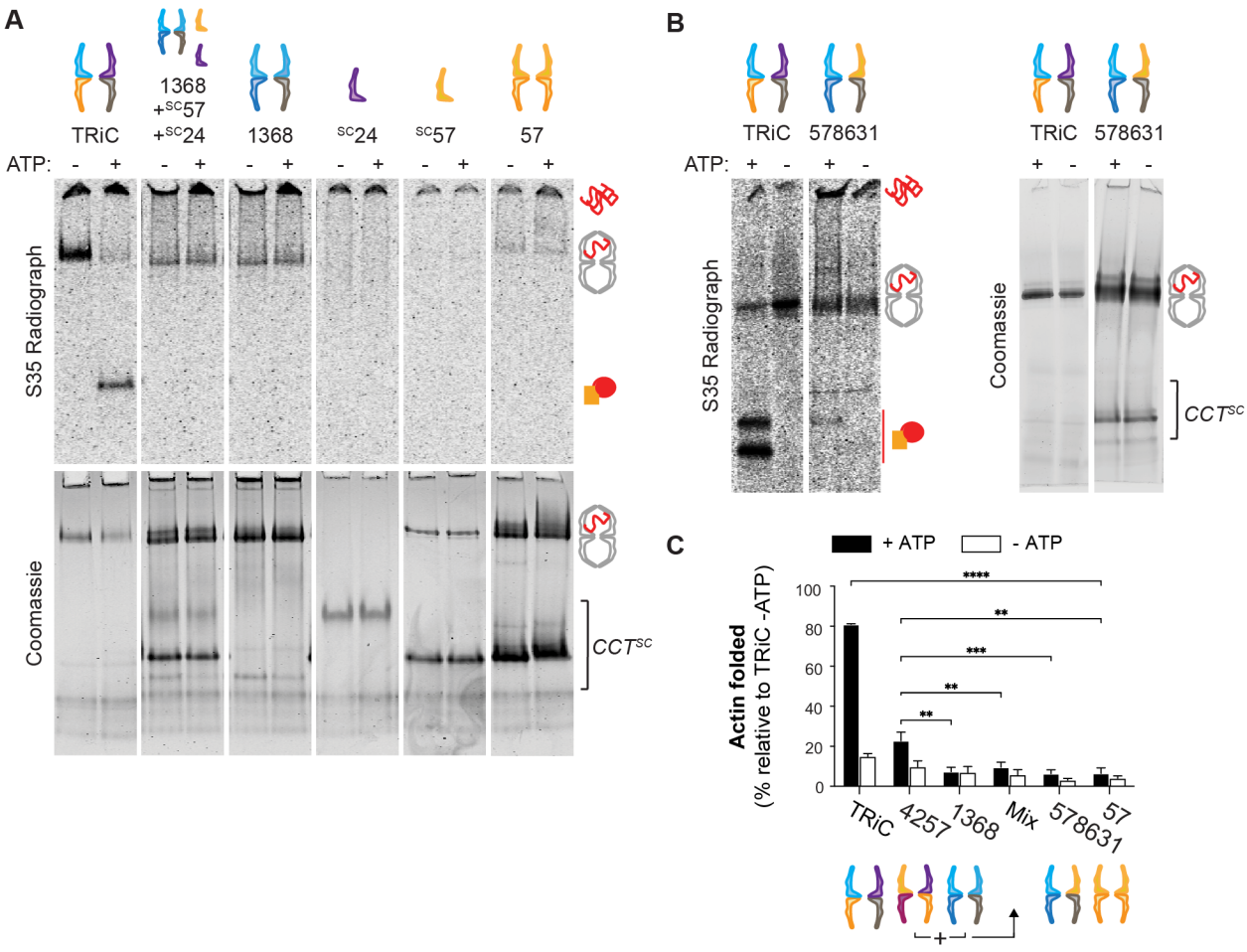

Figure S5. Raw data underlying quantification of actin folding and binding. Related to Figure 5.

A. Representative radiographs for ^{35}S-labeled actin mixed with TRiC or CCT complexes and corresponding NativePAGE. Each sample is a ^{HC}CCT unless otherwise indicated. Samples were analyzed after 1 hour at 30°C +/- ATP. **B.** Identical assay to compare TRiC and ^{HC}CCT578631, carried out on a different day. **C.** Quantification of actin folded by each complex relative to actin bound by TRiC (n = 3). Error bars represent SEM. * $p < 0.05$, ** $p < 0.01$, *** $p < 0.001$, **** $p < 0.0001$, two-way ANOVA, Tukey's multiple comparisons test.

Table S1. Primers used for Cloning and RT-qPCR, related to Star Methods

Gene	Forward Primer	Reverse Primer
HIS-b-actin	GATCTCGAGATGCACCATCATCACCATCACGGCTGCATGGATGATGATATCGCCG	CCCGGTACCCTAGAAGCATTTGCGGTGG
CCT1	CCCATGGGAGAAGTCAAATG	CAAGCAATTTTTGCATTTACGA
CCT2	TTGATATGTCAAGGGTTCAAGATG	GCTGCTAAAACGGTAACAGAGG
CCT3	GACAGACAATAATCGCATTGCT	TGCTCCTGTTCCAACATCAT
CCT4	GAGCATTCTGAAAATAGATGATGTG	CACCAAGGTGATCTTCTTCCA
CCT5	ATTGGAGATGGAACCACAGG	TGAATGCCTCGGTCTAGCA
CCT6	ATGTGCTGCTTCACGAAATG	CATTAGAAGTCGTACCATCACCAG
CCT7	ATTCGAGCTTTCCGCACA	CAGCTTCCTCTGCTCCACTT
CCT8	GTCGCGTGAACTGCTTCC	GCCTCTTCTAATCCTGAAAAGTGT
GAPDH	AGGGCTGCTTTTAACTCTGGT	CCCCACTTGATTTTGGAGGGA

References

1. Chen, J., Sawyer, N., and Regan, L. (2013). Protein-protein interactions: general trends in the relationship between binding affinity and interfacial buried surface area. Protein Sci. 22, 510–515.